JOURNAL OF CATALYSIS 42, 435–442 (1976)

A Molecular-Orbital Investigation of Olefin Insertion Catalyzed by Chromocene on Silica

D. R. ARMSTRONG, R. FORTUNE, AND P. G. PERKINS

Department of Pure and Applied Chemistry, University of Strathclyde,
Glasgow G1 1XL, Scotland

Received August 27, 1975

Modified CNDO/2 and INDO molecular-orbital methods have been used to study the insertion of ethylene into a chromium–hydrogen bond. The reaction sequence under investigation represents a propagation step in the polymerization of an olefin catalyzed by chromocene deposited on a silica surface. The reaction path envisaged is correlated with related reaction mechanisms and the general features common to other reactions of this type are discussed. The two theoretical techniques employed are compared and their physical validity examined.

INTRODUCTION

Subsequent to the recognition of the diverse range of catalytic routes to commercially important materials, the development of optimum catalyst systems has constituted a major area of research (*1, 2*). The important role of transition metal complexes in such reactions has led to the systematic investigation of numerous metal complexes for their potential catalytic activity (*3–6*). Consequently many such reactions are now documented and detailed experimental study has partially elucidated the basic chemical principles involved. The implementation of qualitative theoretical considerations (*5*, *7*, *8*), primarily based on metal–ligand bonding schemes, has further clarified the nature of these catalytic reactions, and proposed reaction sequences, derived from experimental data, are in essential agreement with these approximate bonding patterns. However, despite the growing recognition that calculation can afford a realistic physical description of the electronic nature of reaction paths, more detailed theoretical analysis remains severely restricted. The complexity and magnitude of the problems involved in the direct calculations of reaction coordinates at present preclude the use of rigorous theoretical techniques. Nevertheless, semiquantitative calculations are possible and recently have dealt with symmetry-forbidden-to-allowed catalysis (*5*) and molecular-orbital (MO) studies of the Ziegler–Natta polymerization (*9–11*) and Wacker processes (*12, 13*). In addition, calculations on insertion reactions of hydrido-platinum (II) complexes (*14*) have shown that a modified CNDO/2 computational framework provides an adequate interpretation of such reactions. Since more sophisticated theoretical methods may be employed for complexes of the first-row transition metal ions, the polymerization of ethylene by chromocene deposited on a silica surface (*15*) has been selected for further study.

METHOD

The reaction coordinate studied involved insertion of coordinated ethylene into the

Cr–H bond as shown in Fig. 1. This is a model for a more general insertion process (*15*) in which the H atom is replaced by a ligand R. In the latter case the deposition of chromocene on silica is considered to result in a complex of type (1).

The evident coordinate unsaturation of the chromium atom in this environment is common to many reactions of this type and allows the addition of an olefin to give a complex of type (2): subsequent insertion of the olefin into the Cr–C bond represents the propagation step of the reaction. Termination of the polymerization finally occurs by hydrogen chain-transfer.

The Slater–Condon parameters (*16*) are readily available for first-row transition metal species and hence we were able to compare the INDO (*17*) with the CNDO/2 (*18*) method in tackling such a problem. The modifications to these basic methods employed in the present work facilitate extension of existing parameterization schemes to complexes of the heavier transition metal ions. Owing to the difficulty of obtaining spectral information pertaining to the negative metal atoms, and hence the electron affinities of the metal valence-shell electrons, it is preferable to replace the electronegativities by valence-shell ionization potentials when computing the diagonal elements of the initial H matrix. In this respect the parameterization scheme follows the spirit of the original CNDO/1 formalism (*19*). In addition, the Wolfsberg–Helmholtz approximation (*20*), which was used to estimate the off-diagonal H matrix elements, precludes the lengthy parameterization studies which are necessary when conventional bonding parameters are used. That these alterations do not detract from the overall accuracy of the method has previously been demonstrated in several instances (*9, 12, 14*).

Transference of these modifications to the INDO calculations is accompanied by changes in the evaluation of the core-matrix elements U_{ii}; these differ from those specified in previous calculations. The modifications to U_{ii} result from the more complicated equations involving the energies of outer electronic configurations and the Slater–Condon parameters. Corrections to the one-center Coulomb and exchange integrals relative to F_{ss}^0, chosen as the value of the two-electron one-center integral $\gamma_{ss} = \gamma_{pp} = \gamma_{dd} = 10.55$ eV, are listed in Appendix I. These integrals were calculated from the Slater–Condon parameters derived from spectral sources given in Ref. (*21*). The INDO parameters for the other elements (C, Si, and O) were abstracted from Refs. (*17*) and (*22*).

Bond lengths were taken from standard texts (*23*), the Cr–Cp distance is given in Ref. (*24*), and the initial chromium–hydrogen bond distance was estimated as 0.16 nm. Six steps were considered in the

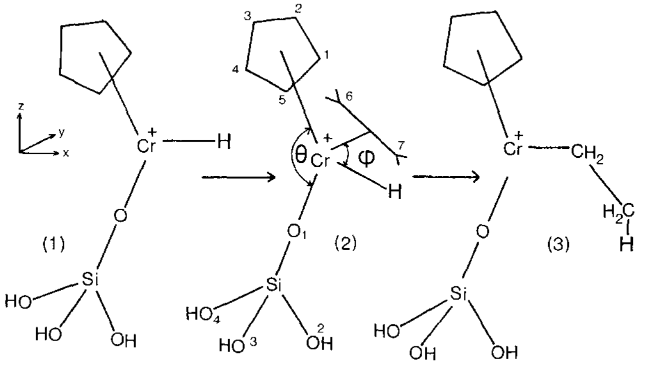

FIG. 1. Insertion of ethylene into the Cr–H bond.

overall reaction sequence (Fig. 2): starting with complex (2) (Fig. 1) the carbon-carbon bond was uniformly increased from "double-bond" to "single-bond" length while concomitant migration of the chromium hydrogen atom was effected. Since experimental evidence demonstrates the bonding of the chromium atom to only one oxygen of the silica surface, this is simulated by the H_3SiO_4 group. The local environment of the chromium atom in complex (2) was assumed to be D_{2d}. Next the angle ϕ was set at 90° and the angle θ was optimized by calculation. The latter angle was found to be ca. 130° and was maintained at this value throughout the reaction coordinate. Although the results obtained clearly refer to the choice of the reaction path, we believe that the gross effects revealed in this investigation apply to any plausible reaction path.

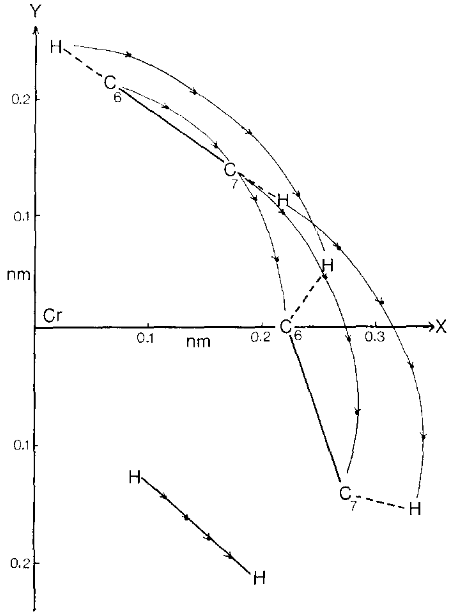

FIG. 2. Reaction coordinate for ethylene insertion.

RESULTS AND DISCUSSION

The electronic features of the reaction path derived from the modified CNDO/2 calculations are summarized in Table 1. Atom charges, bond indices, and partial bond indices are used in discussion of the electronic distribution. The bond indices have previously been defined and their compatibility with chemical intuition demonstrated (*25*, *26*). The "double-bond" of the free ethylene molecule corresponds to a C–C bond index of 2.0. The partial bond index, $P_{\lambda B}$, as the name implies, represents a component of the total index and is defined by

$$P_{\lambda B} = \sum_{\sigma} P_{\lambda\sigma}^2,$$

where the orbitals λ and σ are centered on atoms A and B, respectively. $P_{\lambda B}$ therefore measures the extent to which the orbital contributes to the total bonding between these two atoms.

It should be noted that, in Table 1, where the atoms are not symmetry related but are close to being electronically equivalent (e.g., O_2, O_3, and O_4), data relevant to only one of these atoms are quoted.

Before discussion of the reaction coordinate in detail it is pertinent to examine the nature of the bonding in complex (2). The most striking feature of the electronic distribution is the essential neutrality of the formally dipositive chromium atom (Cr $s^{0.38}$ $p^{0.60}$ $d^{4.95}$). The additional electronic charge is distributed throughout the chromium valence orbitals, with the occupation of the formally vacant s and p orbitals accounting for approximately 50% of this extra electron density. This accumulation of charge is indicative of substantial interaction of this atom with the coordinated ligands. The silicon atom bears a large positive charge stemming from the prevailing polar character of the silicon–oxygen bonds. The oxygen atom which is directly coordinated to the metal carries a considerably lower charge than its counterparts in the silicate network and this, in conjunction with the reduced Si–O_1 bond index and the strong Cr–O_1 bond, leads to substantial Cr–O_1–Si bonding. Therefore, once deposi-

TABLE 1

Electronic Properties for Reaction Coordinate (CNDO)

Atom charges

Step	Cr	Si	O_1	O_2	C_1	C_6	C_7	H
1	+0.070	+1.288	−0.246	−0.347	−0.062	−0.088	−0.019	−0.119
2	+0.085	+1.288	−0.228	−0.355	−0.050	−0.070	−0.006	−0.121
3	+0.084	+1.287	−0.222	−0.354	−0.041	−0.071	+0.017	−0.111
4	+0.075	+1.287	−0.230	−0.355	−0.037	+0.035	+0.036	−0.057
5	+0.062	+1.286	−0.241	−0.356	−0.020	−0.016	−0.007	+0.038
6	+0.070	+1.286	−0.240	−0.356	−0.005	−0.010	−0.082	+0.106

Bond indices

Step	Cr–O_1	Cr–C_1	Cr–C_6	Cr–C_7	Cr–H	Si–O_1	Si–O_2
1	0.746	0.186	0.186	0.266	0.705	0.509	0.863
2	0.736	0.202	0.221	0.213	0.686	0.495	0.870
3	0.734	0.206	0.290	0.177	0.632	0.491	0.873
4	0.736	0.199	0.455	0.150	0.467	0.498	0.873
5	0.742	0.194	0.649	0.117	0.179	0.509	0.872
6	0.748	0.201	0.663	0.082	0.056	0.507	0.872

Step	Cr–C_2	C_6–C_7	Cr–C(Cp)(av)	C–C(Cp)(av)	C_7–H
1	1.313	1.773	0.245	1.287	0.025
2	1.354	1.783	0.263	1.294	0.045
3	1.361	1.712	0.269	1.298	0.109
4	1.314	1.475	0.264	1.301	0.338
5	1.263	1.162	0.264	1.302	0.742
6	1.261	1.060	0.266	1.302	0.892

Atomic orbital occupancies

Step	s	p_x	p_y	p_z	$d_{x^2-y^2}$	d_{xz}	d_{z^2}	d_{yz}	d_{xy}
1	0.377	0.200	0.226	0.172	1.849	1.110	0.463	0.543	0.989
2	0.368	0.208	0.239	0.171	1.852	1.258	0.386	0.482	0.950
3	0.345	0.209	0.246	0.171	1.522	1.308	0.421	0.589	1.105
4	0.312	0.201	0.228	0.170	1.433	1.291	0.434	0.564	1.282
5	0.290	0.191	0.178	0.169	1.448	1.229	0.634	0.510	1.289
6	0.282	0.189	0.150	0.167	1.279	1.080	0.693	0.778	1.311

tion of the chromocene on the silica surface is accomplished, the strength of the metal–silicate interactions virtually precludes the reverse process and permits the ensuing polymerization reaction to take place.

Electron density withdrawn from the cyclopentadienyl (Cp) ring system contributes to the electron density associated with the metal atom and ensures relatively strong metal–ring interaction. It is interesting to note that this metal–ligand bonding is slightly weakened by comparison with chromocene itself. The decrease in bond index, which is opposite to that expected for a C_{2v} distortion of chromocene (*27*), emphasizes the importance of attachment of chromium to the silica surface. The ethylene moiety is more loosely bound to the metal than is the Cp ring system although the reduced olefinic C_6–C_7 bond index of 1.773 indicates the existence of the classical σ–π synergic bonding situation (*28*).

The ensuing ethylene insertion is energetically favored and this is the driving force of the reaction. The reaction sequence

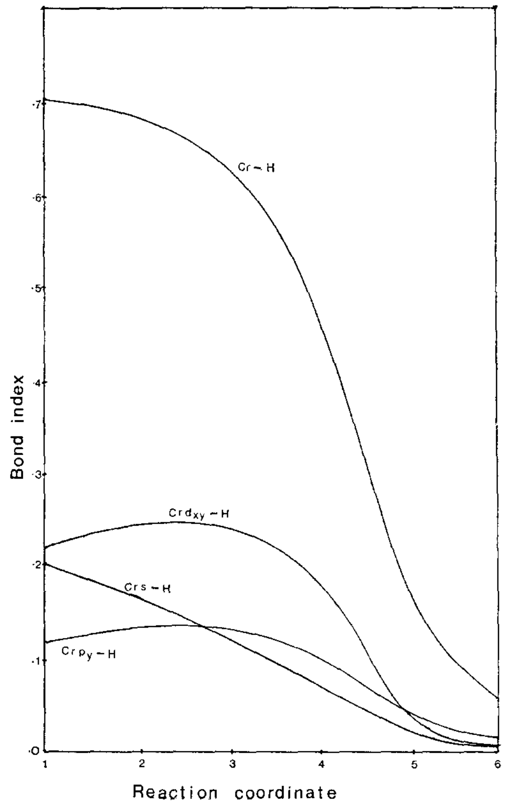

FIG. 3. Bond index variation for the Cr–H bond along the reaction coordinate.

is characterized by decreasing carbon–carbon double-bond character accompanied by a concomitant increasing Cr–C_6 bond strength as the insertion proceeds. Bonding of the chromium to both the Cp ring and the silicate surface marginally increases, in compensation for the Cr–H bond weakening. The enhanced stability of the product may be largely attributed to the Cr–C_6 and C–H σ-bond formation.

Closer inspection of Table 1 clearly demonstrates the complex balance achieved between bond formation and bond breaking. At each stage of the reaction the ethylene and hydrogen are bonded to chromium and so no energy is needed for bond breaking. The bond weakening which occurs is more than compensated by the formation of the new bonds. Prior to σ-bond formation the metal–ethylene bonding is principally due to interaction with the metal d_{xy} orbital. Similarly, the metal–hydrogen bonding is dominated by metal d_{xy} orbital interaction, although the chromium s and p orbital contributions are not negligible. The essential function of the metal d_{xy} orbital in the insertion reaction merits further comment and, for this purpose, reference is made to the changes in the partial bond indices for selected bonded interactions (Figs. 3 and 4). As the reaction proceeds, increasing d_{xy}–C_6 and d_{xy}–H interactions illuminate the role of this orbital as a transfer agent. This permits a smooth transition between the related bonding patterns characteristic of reactant and product. In the later stages of the reaction the Cr–C_6 and the C–H σ-bonds

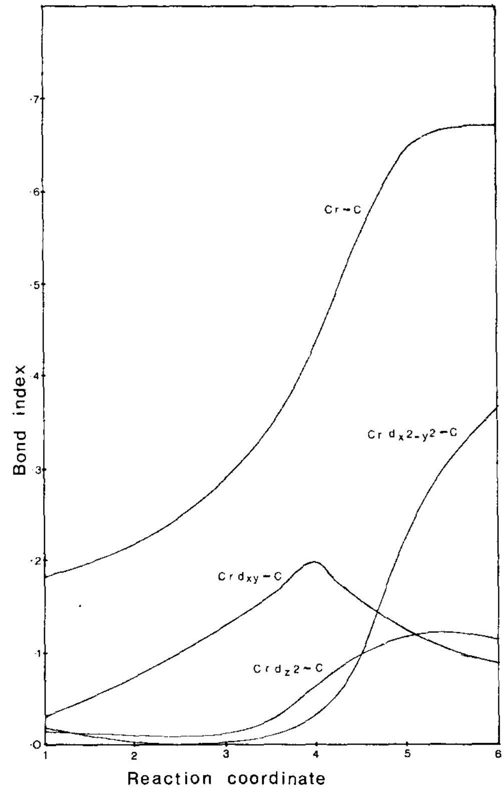

FIG. 4. Bond index variation for the Cr–C_6 bond along the reaction coordinate.

TABLE 2

Electronic Properties of Reaction Coordinate (INDO)

Atom charges

Step	Cr	Si	O_1	O_2	C_1	C_6	C_7	H
1	+0.084	+1.426	−0.362	−0.427	−0.021	−0.058	+0.023	−0.131
2	+0.115	+1.426	−0.350	−0.425	−0.007	−0.044	−0.030	−0.146
3	+0.106	+1.427	−0.345	−0.424	+0.004	−0.044	+0.051	−0.136
4	+0.088	+1.426	−0.349	−0.425	+0.005	−0.044	+0.079	−0.096
5	+0.059	+1.425	−0.370	−0.428	−0.004	+0.014	+0.041	+0.013
6	+0.061	+1.425	−0.360	−0.426	+0.002	+0.020	−0.034	+0.086

Bond indices

Step	$Cr-O_1$	$Cr-C_1$	$Cr-C_6$	$Cr-C_7$	Cr-H	$Si-O_1$	$Si-O_2$
1	0.826	0.241	0.208	0.267	0.757	0.564	0.838
2	0.830	0.269	0.235	0.220	0.730	0.554	0.844
3	0.841	0.278	0.293	0.188	0.660	0.550	0.847
4	0.840	0.273	0.491	0.163	0.516	0.556	0.828
5	0.845	0.197	0.740	0.119	0.190	0.577	0.842
6	0.844	0.187	0.748	0.086	0.060	0.567	0.827

Step	C_1-C_2	C_6-C_7	Cr-C(Cp)(av)	C-C(Cp)(av)	C_7-H
1	1.274	1.792	0.276	1.288	0.015
2	1.332	1.796	0.302	1.290	0.031
3	1.376	1.733	0.306	1.292	0.087
4	1.367	1.492	0.314	1.293	0.312
5	1.325	1.157	0.318	1.295	0.752
6	1.305	1.070	0.315	1.294	0.900

Atomic orbital occupancies for chromium

Step	s	p_x	p_y	p_z	$d_{x^2-y^2}$	d_{xz}	d_{z^2}	d_{yz}	d_{xy}
1	0.382	0.198	0.223	0.171	1.793	0.941	0.624	0.970	0.613
2	0.376	0.207	0.241	0.171	1.839	1.066	0.548	0.843	0.593
3	0.351	0.208	0.251	0.170	1.384	1.124	0.518	0.964	0.923
4	0.318	0.199	0.233	0.170	1.283	1.111	0.500	0.929	1.168
5	0.302	0.186	0.174	0.169	1.443	1.012	0.974	0.676	1.006
6	0.296	0.184	0.145	0.167	1.228	0.927	0.897	0.993	1.102

become established, and the presence of a transfer orbital is no longer required. Consequently the d_{xy}–C_6 interaction is replaced by the stronger $d_{x^2-y^2}$–C_6 interaction. The important complementary functions of the metal $d_{x^2-y^2}$ and the d_{xy} orbitals are reflected by their respective loss and gain of electron density. It may also be noted that the large reduction in Cr–C_1 bond index with respect to the average for the Cr–C(Cp) bonds is accounted for by the lessening of the initial Cr($d_{x^2-y^2}$)–C_1 interaction.

The electronic properties calculated at the INDO level of approximation are summarized in Table 2. A cursory examination of this table is sufficient to establish the complete compatibility of the two calculational procedures. However, differences do exist, and a comparison of these with respect to complex (2) is adequate to highlight the major points. The INDO calculations induce further localization of electron density on the metal atom. This in turn gives rise to more powerful metal–ligand interactions as shown by the higher Cr–C_1, Cr–O, and

Cr–H bond indices. The positive charge on the silicon is increased as is also the Si–O_1 bond index. The latter demonstrates the enhanced Cr–O_1–Si bonding at the expense of Si–$O_{2,3,4}$ bonding. The additional electron density associated with the chromium atom is localized principally in the d_{z^2} and d_{yz} orbitals, a diminution of electron density being evident in the other d orbitals. Overall, d-orbital participation in the bonding becomes stronger.

The electronic rearrangements occurring with each successive step of the reaction coordinate closely resemble those revealed by CNDO calculations. This similarity between the CNDO and INDO results throughout the reaction path renders detailed discussion redundant, and it suffices to record that the stronger metal–ligand bonding which is characteristic of the INDO calculation on the reactant (2) is manifest throughout the reaction sequence. In both sets of calculations we find that the migrating hydrogen is essentially electrically neutral. This agrees with previous work on comparable insertion processes where the migrating hydrogen was found to bear a slight negative charge (*14*).

It is of final interest to note that, despite the expected disparity in total energies evaluated by the two computational procedures, the energy differences between reactant and product are almost identical. This substantiates the view that, while such semi-empirical techniques are far from rigorous in absolute terms, their effectiveness in comparative studies of related chemical species justifies their continued use.

In conclusion, we emphasize that the "transfer orbital" is definitive of catalyst systems of this type. The principal function of the metal is to provide such a transfer medium and in this context the domination of Zeigler–Natta catalyst systems by metals near the onset of the first transition series is readily rationalized. One prerequisite of an accessible transfer system is the ready disposition of the d orbitals to modulate electronic reorganization. This task is more difficult if, as in the case of metals of the nickel triad, the d-orbital occupancies approach saturation.

It is also apparent that both the CNDO and INDO molecular-orbital methods produce a physically reasonable interpretation of the electronic properties of reaction pathways. The two techniques are complementary, the major difference arising from inclusion of the additional one-center two-electron integrals is the enhanced metal–ligand bonding.

APPENDIX I

CORRECTIONS TO THE ONE-CENTER COULOMB AND EXCHANGE INTEGRALS FOR CHROMIUM

	s	p_x	p_y	p_z	$d_{x^2-y^2}$	d_{xz}	d_{z^2}	d_{yz}	d_{xy}
s	0.0	0.0114	0.0114	0.0114	0.0072	0.0072	0.0072	0.0072	0.0072
p_x	0.0	0.0047	0.0036	0.0036	0.0073	0.0073	0.0031	0.0010	0.0073
p_y	0.0	−0.0024	0.0047	0.0036	0.0073	0.0010	0.0031	0.0073	0.0073
p_z	0.0	−0.0024	−0.0024	0.0047	0.0010	0.0073	0.0056	0.0073	0.0010
$d_{x^2-y^2}$	0.0	0.0050	0.0050	−0.0100	0.0308	0.0207	0.0024	0.0207	0.0118
d_{xz}	0.0	0.0050	−0.0100	0.0050	−0.0107	0.0308	0.0148	0.0207	0.0207
d_{z^2}	0.0	−0.0050	−0.0050	0.0100	−0.0167	0.0013	0.0308	0.0148	0.0237
d_{yz}	0.0	−0.0100	0.0050	0.0050	−0.0107	−0.0107	0.0013	0.0308	0.0207
d_{xy}	0.0	0.0050	0.0050	−0.0100	0.0072	−0.0107	−0.0167	−0.0107	0.0308

Since the identities $(\mu\mu|\nu\nu) = (\nu\nu|\mu\mu)$ and $(\mu\nu|\mu\nu) = (\nu\mu|\nu\mu)$ hold, where μ and ν are atomic orbitals on the metal, the INDO corrections to the one-center Coulomb integral $\gamma_{\mu\mu} = (\mu\mu|\mu\mu)$ are given in the lower triangle of the above matrix while the one-center exchange integrals $(\mu\nu|\mu\nu)$ are given in the upper triangle of the matrix; all are in atomic units.

ACKNOWLEDGMENT

One of us (R. F.) thanks the University of Strathclyde for a bursary.

REFERENCES

1. Hartley, F. R., "The Chemistry of Platinum and Palladium." Applied Science Publishers, London, 1973.
2. Schrauzer, G. N., "Transition Metals in the Homogeneous Catalysis." Marcel Dekker, New York, 1971.
3. Bailey, G. C., *Catal. Rev.* **3**, 37 (1969).
4. Schrauzer, G. N., *Advan. Catal.* **18**, 373 (1968).
5. Mango, F. D., *Advan. Catal.* **20**, 291 (1969).
6. Orchin, M., *Advan. Catal.* **16**, 1 (1966).
7. Mango, F. D., and Schachtschneider, J. H., *in* "Transition Metals in Homogeneous Catalysis" (G. N. Schrauzer, Ed.), Chap. 6, Marcel Dekker, New York, 1971.
8. Mango, F. D., and Schachtschneider, J. H., *J. Amer. Chem. Soc.* **89**, 2484 (1967).
9. Armstrong, D. R., Perkins, P. G., and Stewart, J. J. P., *J. Chem. Soc. Dalton*, 1972 (1972).
10. Cossee, P., *J. Catal.* **3**, 80 (1964).
11. Armstrong, D. R., Perkins, P. G., and Stewart, J. J. P., *Rev. Roum. Chim.* **19**, 1695 (1974).
12. Armstrong, D. R., Fortune, R., and Perkins, P. G., to be published.
13. Sakaki, S., Hato, H., Kanai, H., and Tarama, K., *Bull. Chem. Soc. Jap.* **47**, 377 (1974).
14. Armstrong, D. R., Fortune, R., and Perkins, P. G., *J. Catal.* **41**, 51 (1976).
15. Karol, F. J., Karapinka, G. L., Wu, C., Dow, A. W., Johnson, R. N., and Carrick, W. L., *J. Polym. Sci.* **10A**, 2621 (1972).
16. Slater, J. C., "Quantum Theory of Atomic Structure," Vol. 1. McGraw-Hill, New York, 1960.
17. Pople, J. A., Beveridge, D. L., and Dobosh, P. A., *J. Chem. Phys.* **47**, 2026 (1967).
18. Pople, J. A., and Segal, G. A., *J. Chem. Phys.* **44**, 3289 (1966).
19. Pople, J. A., and Segal, G. A., *J. Chem. Phys.* **43**, *s* 736 (1965).
20. Wolfsberg, M., and Helmholtz, L., *J. Chem. Phys.* **20**, 837 (1952).
21. Tondello, E., De Michelis, G., Oleari, L., and Di Sipio, L., *Coord. Chem. Rev.* **2**, 65 (1967).
22. Benson, H. G., and Hudson, A., *Theor. Chim. Acta* **23**, 259 (1971).
23. "Interatomic Distances in Molecules and Ions," *Chem. Soc. Special Publ.*, No. 11, London, 1958.
24. Weiss, E., and Fischer, E. O., *Z. Anorg. Allgem. Chem.* **284**, 69 (1956).
25. Armstrong, D. R., Perkins, P. G., and Stewart, J. J. P., *J. Chem. Soc. Dalton*, 838 (1973).
26. Armstrong, D. R., Perkins, P. G., and Stewart, J. J. P., *J. Chem. Soc. Dalton*, 2273 (1973).
27. Armstrong, D. R., Fortune, R., and Perkins, P. G., to be published.
28. Chatt, J., Duncanson, L. A., and Venanzi, L. M., *J. Chem. Soc.*, 4456 (1955).